Behavior of the aggregate wind resource in the ISO regions in the United States *

Udaya Bhaskar Gunturu and C. Adam Schlosser

The MIT Joint Program on the Science and Policy of Global Change combines cutting-edge scientific research with independent policy analysis to provide a solid foundation for the public and private decisions needed to mitigate and adapt to unavoidable global environmental changes. Being data-driven, the Program uses extensive Earth system and economic data and models to produce quantitative analysis and predictions of the risks of climate change and the challenges of limiting human influence on the environment—essential knowledge for the international dialogue toward a global response to climate change.

To this end, the Program brings together an interdisciplinary group from two established MIT research centers: the Center for Global Change Science (CGCS) and the Center for Energy and Environmental Policy Research (CEEPR). These two centers—along with collaborators from the Marine Biology Laboratory (MBL) at Woods Hole and short- and long-term visitors—provide the united vision needed to solve global challenges.

At the heart of much of the Program's work lies MIT's Integrated Global System Model. Through this integrated model, the Program seeks to: discover new interactions among natural and human climate system components; objectively assess uncertainty in economic and climate projections; critically and quantitatively analyze environmental management and policy proposals; understand complex connections among the many forces that will shape our future; and improve methods to model, monitor and verify greenhouse gas emissions and climatic impacts.

This reprint is one of a series intended to communicate research results and improve public understanding of global environment and energy challenges, thereby contributing to informed debate about climate change and the economic and social implications of policy alternatives.

Ronald G. Prinn and John M. Reilly,
Program Co-Directors

Behavior of the aggregate wind resource in the ISO regions in the United States

CrossMark
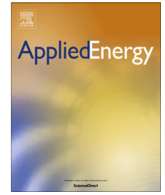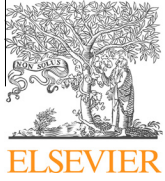
Udaya Bhaskar Gunturu [a,b,*], C. Adam Schlosser [a]

[a] The MIT Joint Program on the Science and Policy of the Global Change, Massachusetts Institute of Technology, Cambridge, MA 02139, USA
[b] King Abdullah University of Science and Technology, Thuwal 23955-6900, Saudi Arabia

HIGHLIGHTS

- Aggregated wind power in the ISO regions in the US has been studied.
- Aggregation mitigates intermittency partially.
- The intermittency in power generation is synchronized spatially in each region.
- The benefits of aggregation saturates asymptotically with the number of generating units.
- The benefits of aggregation falls with the correlation between the generating units.

ARTICLE INFO

ABSTRACT

The collective behavior of wind farms in seven Independent System Operator (ISO) areas has been studied. The generation duration curves for each ISO show that there is no aggregated power for some fraction of time. Aggregation of wind turbines mitigates intermittency to some extent, but in each ISO there is considerable fraction of time when there is less than 5% capacity. The hourly wind power time series show benefit of aggregation but the high and low wind events are lumped in time, thus indicating that intermittency is synchronized in each region. The timeseries show that there are instances when there is no wind power in most ISOs because of large-scale high pressure systems. An analytical consideration of the collective behavior of aggregated wind turbines shows that the benefit of aggregation saturates beyond a certain number of generating units asymptotically. Also, the benefit of aggregation falls rapidly with temporal correlation between the generating units.

© 2015 Published by Elsevier Ltd.

1. Introduction

As the United States considers increasing the proportion of wind power to 20–30% of its total generation capacity by 2030 [1], the primary hurdle is the intermittency of wind power and its integration into the electric grid to improve wind reliability, cost effectiveness and performance [2]. The two main consequences of intermittency are rapid loss or gain of power (high ramp rates) and durations without power or with very low power (also called loss of load) [3]. Geographical diversification of wind farms, with the inherent assumption that the fluctuations would be smoothed by such aggregation, has been recommended as an effective strategy to obtain steady wind power [4,5].

An inherent assumption in this strategy is the instantaneous spatial inhomogeneity of wind resource. Geographic diversification steadies wind power in the time scales of millisecond to minute and hence renders the electric grid more stable [6,3]. The fluctuations in wind at these scales are predominantly random. However, as the time scale of the forces that generate the fluctuations increases, so does the spatial scale of these fluctuations – due in large part by the associated synoptic-scale (i.e. 500–1000 km scale) meteorological systems. Thus, the fluctuations in wind speed are presumably coherent over large spatial and temporal scales.

Mitigation of wind variability is essential for its efficient integration into the power grid [3,7]. Geographically and electrically, the balancing areas need to be large for accommodating the variability characteristics of wind power like ramping behavior and intermittency. Proximity and access to flexible conventional generation, as well as maneuverability are essential for managing the variability in wind generation. Since most of these requirements are efficiently fulfilled by the Independent System Operator

Table 1
The ISO regions.

Abbreviation	ISO region
CalISO	California ISO
ERCOT	Electric Regulatory Commission Of Texas
MISO	Midwest ISO
NEISO	New England ISO
NYISO	New York ISO
PJM	Pennsylvania, New Jersey and Maryland ISO
SWPP	SouthWest Power Pool

(ISO) areas, wind integration would essentially occur across a whole ISO region [8].

Although aggregation of power from wind turbines can be conceived at any spatial scale, constraints like cost of laying transmission lines and grid operations practically limit aggregation to the ISO regions [4,8]. Table 1 shows the abbreviations and the areas covered by the different ISO regions shown in map 1. Thus, this essay attempts to describe the statistical and intermittency characteristics of the aggregated power in each of seven ISO regions shown in Fig. 1.

Several researchers and all turbine manufacturers use wind speed as a measure of wind power resource [10]. But the energy density of wind is a function of air density, and the energy density over a plain is greater than that on a mountain (at a presumably higher altitude) for the same wind speed.

Thus, wind power density (WPD) is a more robust representative of wind power resource. Further, a constant air density has been assumed in other works [11]. Non-consideration of the variability in air density results in a minimum potential RMS error of 16% [12].

Earlier studies used wind resource data that was coarse in spatial resolution [13], sparse and uneven in coverage, short in length of the record [14,15], or low temporal resolution [16,17,14]. While the coarse spatial resolution and sparse spatial coverage prevent a realistic description of the resource and its variability, the short lengths of the record do not allow inter-annual variability and the variability due to El-Nino like interannual climate modes of the atmosphere to be taken into account. Moreover, the low temporal resolution does not allow investigation of the impact of the variability on the grid stability (seconds to minutes) or capacity adequacy (1–24 h).

Further, almost all of the earlier wind resource constructions scaled the wind speed from a lower altitude (usually 10 m) to that of the turbine hub height using a constant scaling exponent irrespective of surface roughness. Even in the reanalysis datasets, the wind speeds are computed using pressure gradients and the surface roughness is not taken into account [18].

2. Data and methodology

In view of these considerations, we construct the wind resource in the United States for the present study using a novel approach in which boundary layer parameters, like surface roughness, displacement height and friction velocity are used to compute the wind speed at the hub height (80 m) using similarity theory of the atmospheric boundary layer [19]. The boundary layer parameters are from the Modern Era Retrospective-analysis for Research and Applications (MERRA) reanalysis dataset [20]. An elaboration of the method is given in the Appendix A and a further detailed account in [19]. The domain over which the wind resource was constructed is bounded by 20–50° N and 130–60° W. The
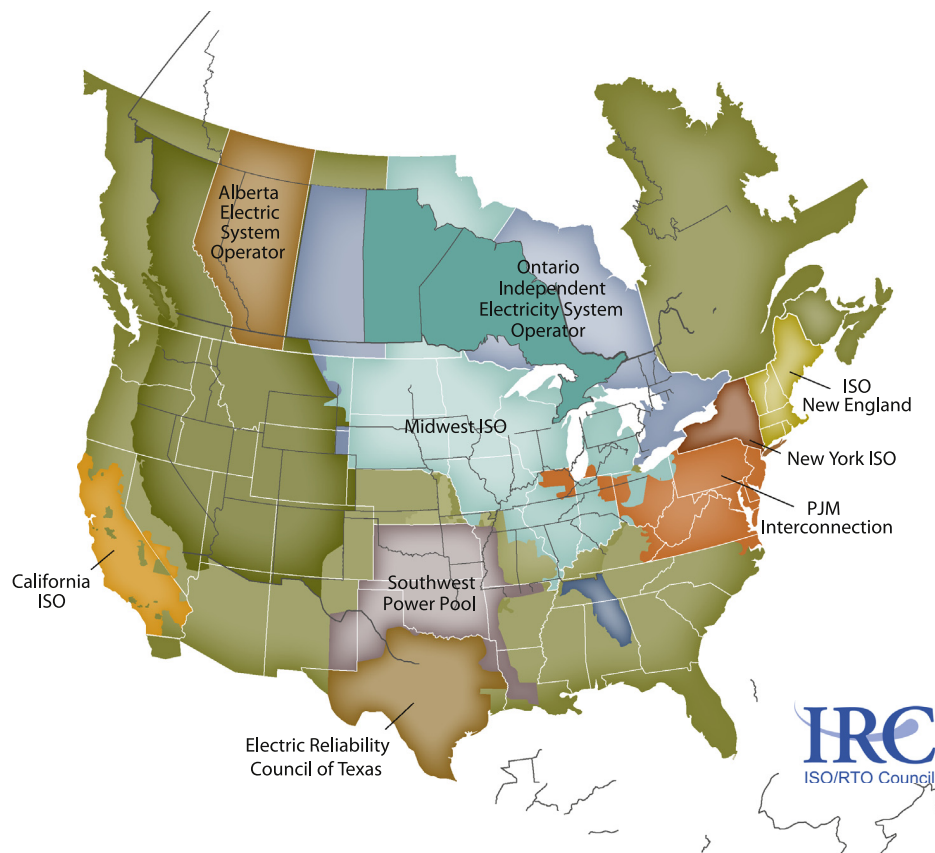

Fig. 1. The map of the different ISOs in the U.S. [9]. It has been shown that wind integration will optimally occur over these ISO regions.
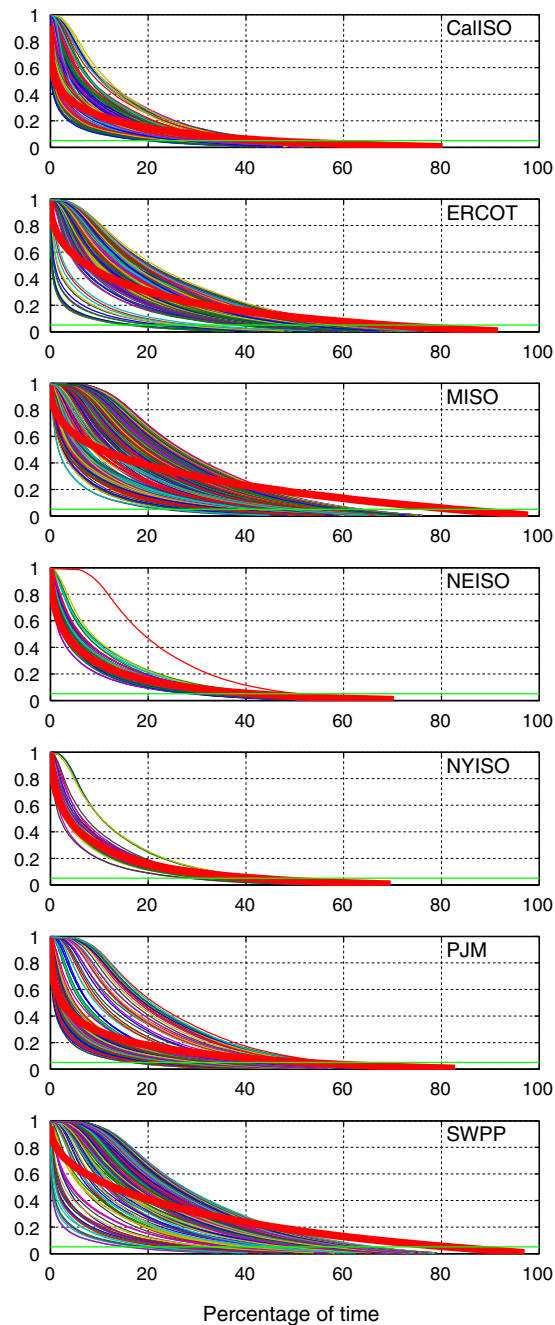
Fig. 2. Power generating profiles of the ISO regions. The panels show the generation duration curves of the individual grid points (thin lines) and the aggregated power in the whole ISO region (thick red). The labels on the panels show the ISO region. The abscissa is the percentage of time during the 31 years of data considered and the *y*-axis is the capacity factor. (For interpretation of the references to color in this figure legend, the reader is referred to the web version of this article.)

spatial resolution of the wind speed dataset is 1/2° latitude × 2/3° longitude.

WPD is computed using the instantaneous air density and the wind speed at an 80 m hub height. Assuming deployment of GE 1.5xle turbine whose power conversion curve is given in the Appendix A, and an optimum spacing of the turbines to minimize wake effects [21], the power generated at each hour is computed at each grid point. The capacity factor of each grid point is computed as the ratio of the total power generated during the 31 years. Although it is assumed that 1% of the grid cell area is used for wind turbine deployment, since this study considers variables that are

ratios, the fraction of area of deployment is rendered extraneous for the sake of arguments in this study.

3. Generation duration curves

Generation duration curves are an important tool in power engineering to understand the generating profile of power plants [14,15]. In a generation duration curve, the inverse cumulative probability distribution of the generated power is plotted as a function of the percentage of time in a year that the generation is greater than or equal to the ordinate generation. In Fig. 2, the generation as a fraction of the rated power (capacity factor) is plotted for each ISO. The aggregated capacity factor (ACF) of the whole ISO region (computed as the ratio of the total power generated and the total installed power in the ISO region) is also plotted as the red curve.

Although aggregation of wind power in each ISO increases the duration for which the ACF is above 0.05 (5% of the maximum), there remains a sizeable percentage of time (from 15% to as much as 60%) in each ISO for which the ACF is below 0.05. Nevertheless, the improvement via aggregation is very noticeable in the case of MISO and SWPP (Table 1). The regions that have less wind resources (California, New England, New York and PJM (Table 1) have longer durations without any power, whereas such durations for the regions that have modest resources (MISO, ERCOT and SWPP (Table 1) are shorter. In a study of the advantages of aggregating wind farms in northeast Texas, Oklahoma and New Mexico (corresponding to the SWPP region), it was reported [14] that an aggregation of 19 sites produced at least 21% of the rated power 79% of the time leading to the conclusion that wind power in that region can be used to supply about 33% of the baseload generation. From the duration curve for SWPP (Fig. 2), the aggregation of all the grid points produces at least 21% of the rated power only 45% of the time. Two important reasons for this difference are that Archer and Jacobson [14] consider wind data only for the year 2000 and extrapolate the wind speed data to 50 m height. The present study considers a longer wind record of 31 years and derives the wind speed at 80 m directly from boundary layer flux parameters. Incidentally, the year 2000 was a La Nina year and the wind speeds were faster than normal. Moreover, we find that our wind resource assessment[19] for the year 2000 had anomalously higher number (13% more than the long term annual mean) of grid points of usable (>200 W/m²) wind power density.

These duration curves are also useful in assessing the integration. In some of the ISOs (ERCOT, MISO, PJM and SWPP), there are some grid points which have a sharply falling duration curve. So, if these grid points are omitted, it is possible to optimize the performance of aggregation.

Table 2 shows the statistics of the intermittent behavior of the aggregated power in these seven ISOs. The table shows the

Table 2
Statistics of intermittency in different ISOs in the U.S.

ISO	Critical hours (%)			Level crossing rate (/yr)		CoV of AP[a]	Median ACF[b]
	< 0%	< 5%	< 10%	5% level	10% level		
CalISO	0.25	53	70	298	263	1.26	0.04
ERCOT	0.1	28	45	239	262	1.02	0.12
MISO	~0	15	30	150	212	0.82	0.18
NEISO	1.8	56	71	198	161	1.51	0.03
NYISO	2.21	56	70	198	160	1.52	0.04
PJM	0.24	45	63	213	189	1.22	0.06
SWPP	~0	17	31	180	238	0.85	0.18

[a] Aggregated power.
[b] Aggregated capacity factor.

percentage of critical hours as a fraction of the total number of hours in each ISO. Here the critical hours are defined as the times when the aggregated power in the ISO is less than or equal to 5% or 10% of the total installed capacity. The level crossing rate shows the number of times the aggregated power crosses a threshold (5% or 10% of the installed capacity). The coefficient of variation of the aggregated power shows its variability. From the statistics in this table, it can be inferred that MISO and SWPP stand out in terms of having the most favorable statistics of aggregate intermittency and capacity factor.

4. Power time series

The power timeseries (Figs. 3) show that there is a general lumping of generation in time such that there are times when almost no power is produced in the whole ISO region. This temporal clustering is predominant in the ISOs in the central USA (MISO, ERCOT and SWPP). The benefit of aggregation is manifested to a greater extent in California ISO. These timeseries also show that the random small scale fluctuations are mostly damped but the longer timescale fluctuations persist even in the aggregate power. These timeseries show that there are times when the whole ISO has insignificant wind generation.

Aggregation of power from different turbines makes the ramp rates large with higher penetration of wind installation. The aggregate curve in the timeseries plots shown is a mean of the power timeseries at the individual grid points. Thus, if that curve is multiplied by the number of grid points in each of the ISO region, the ramp rates may be very steep.

A common question considered in wind integration is if wind stops blowing over a large region at the same time [4]. These illustrative timeseries correspond to the time between 2000 Hrs UTC on 11th January, 1979 and 1600 h UTC on 12th January, 1979. Between 60 and 80 h, there is almost no wind in New England, New York, PJM, MISO and very little wind blew in ERCOT and SWPP. If a high pressure system and a low pressure system are in proximity, the configuration results in high winds from the high to the low pressure. But if a high pressure system is in isolation or if the high and low pressures are far removed from each other, in most cases, it results in low winds. Fig. 4, which shows the mean sea level pressure across the U.S. for this period, indicates that there was a high pressure system over New England and New York and it extended westward and southward such that many ISOs did not have wind resource simultaneously. During these hours, California ISO has some inhomogeneity in wind resource across the grid points. But considering the fact that the wind resource in California is low compared to MISO, ERCOT and SWPP, the wind power in California is unlikely to make up for the lull in the other ISOs.

Phenomena called atmospheric blockings result in high or low pressure systems that persist for several days. Usually, blocking highs that cause persistent and widespread high pressure systems are associated with little or no wind at the surface. The northern Atlantic is a region with high frequency of blockings a mean frequency of 25% of the time [22]. Although the mechanism of formation and maintenance of atmospheric blocking is not understood well, the impacts and the synoptic features are clear. Thus, the frequency of these blockings is not insignificant. These blockings are responsible for multi-ISO wide low wind phenomena. More significantly, the frequency of blockings in the North Atlantic is on the rise with changing climate [23].

5. Analytical treatment of collective behavior

Central to the issue of aggregation is whether there is any asymptotic behavior (i.e. saturation) to the benefits of adding addi-

tional wind farms within a wind-energy collection pool. Earlier work(considering data from 19 wind farms) has suggested that the benefit of aggregation does not saturate with the number of sites [14]. However, in our analysis we find that an important parameter in this assessment is the mean correlation among the aggregated grid points.

Fig. 5 shows the factor by which the coefficient of variation (CoV) is reduced on the ordinate as a function of the number of grid points on the abscissa. The analytical construction of this statistical behavior is presented in the Appendix B. The different curves correspond to
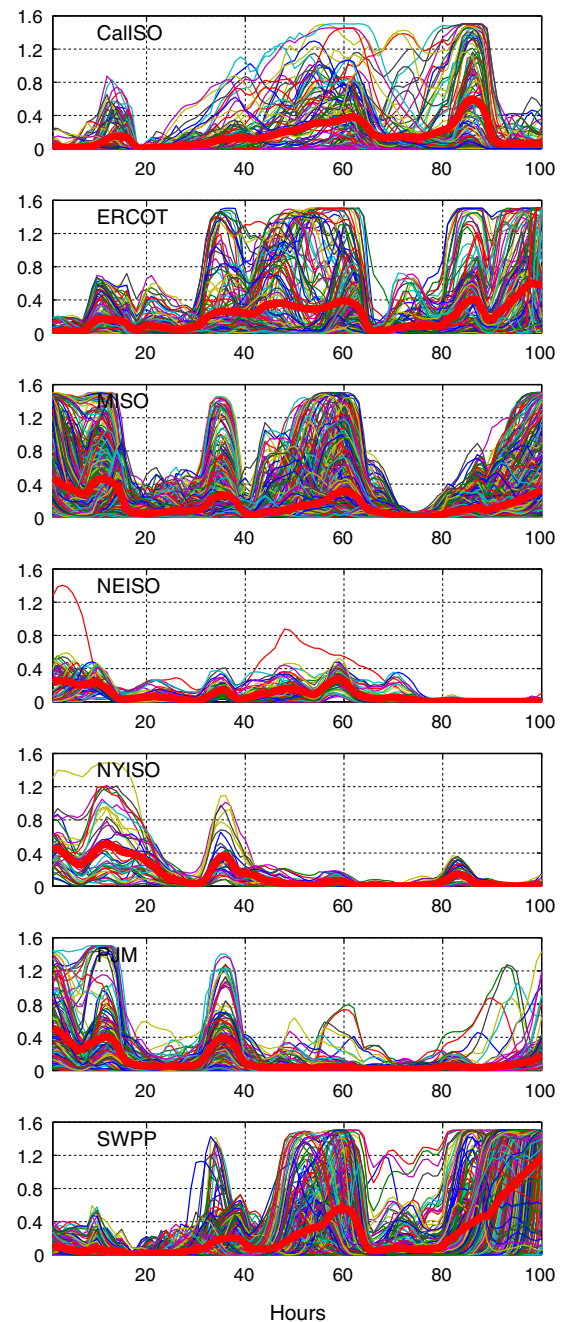

Fig. 3. Illustrative generating profiles. The panels show illustrative time series of the generating profile of the individual grid points in each ISO region (thin lines) and the normalized aggregated power (thick red) for 100 illustrative hours. The *x*-axis shows the hours and the *y*-axis shows the power generated in MW. (For interpretation of the references to color in this figure legend, the reader is referred to the web version of this article.)
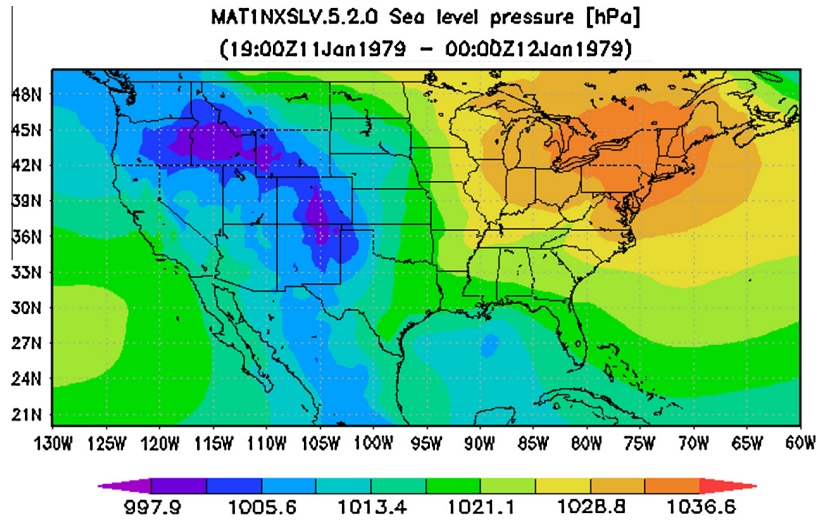
Fig. 4. A high pressure system over a wide area in the eastern and northeastern U.S. The plot shows the mean sea level pressure on 11th and 12th January, 1979. The hours correspond to the hours from 60th to 84th in the plot of the illustrative power time series in the Fig. 3. MERRA [20] dataset has been used for this plot.
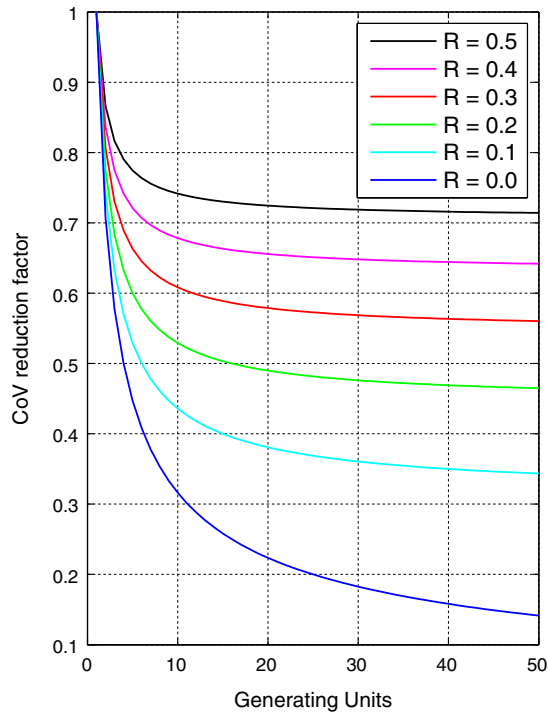

Fig. 5. Variation of CoV with number of aggregated generating units. *R* is the mean coefficient of correlation between the generating units.

different mean correlations (R) as shown in the legend. This plot shows that with no mean correlation, the CoV has a stronger reduction with additional grid points. However, as the mean R among the generating units increases, the impact of increased units on the decay of CoV is reduced. The ratio of the CoV with correlation *R* and without correlation (*R* = 0) asymptotically varies as $\sqrt{R}$ as the number of turbines increases to ∞. Further, this plot also shows that in all cases of *R* considered, the initial 10 units result in the majority of reduction in CoV. For subsequent additional units, the benefit of aggregation is marginal. More importantly, as the correlation between the units increases, the benefit of aggregation saturates faster, that is with fewer number of turbines. Even with a correlation of 0.3, the reduction in the coefficient of variation becomes almost half
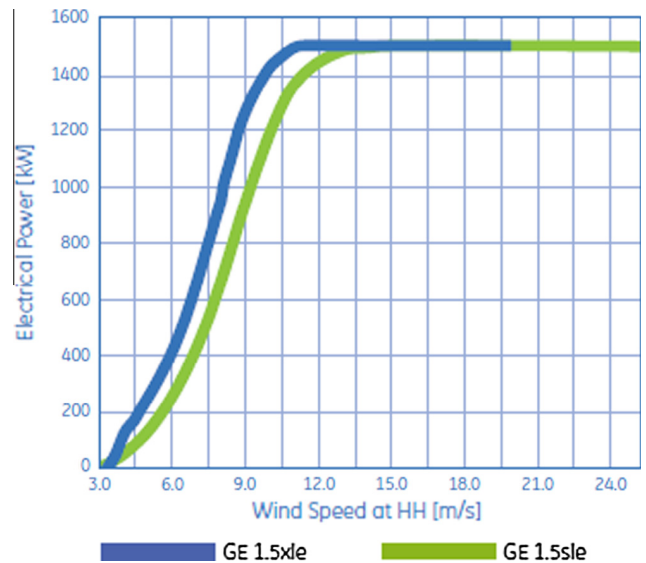

Fig. A.6. Power conversion curve for GE XLE 1.5 MW turbine [28]. The *x*-axis is the wind speed and the curve shows the corresponding power generated in kW.

of that with no correlation. Finally, this saturation depends neither on the nature of the turbine nor the wind resource at the individual locations.

The mean and standard deviation of power generated with and without aggregation presented in an earlier report [14] have been used to compute the mean correlation coefficient in the aggregation considered in that work. The use of the analysis of the collective behavior of the wind power sites results in a mean correlation coefficient of 0.48. The main point here is that the variability of the aggregated wind power, which impacts the power systems detrimentally, is dependent on the magnitude of the correlation of the generating units.

6. Conclusions

The GDC show that in regions with greater WPD (MISO and SWPP), aggregation of the wind power from all grid points noticeably improves the duration for which the aggregated power is

greater than 5% of the maximum whereas in the other ISOs, the improvement is less significant. The power timeseries show that no power is produced during some times in the whole ISO regions. Further, when there are large-scale high pressure systems, several ISO regions do not have any power.

The analytical treatment of the ratio of coefficient variation of wind power with and without aggregation as a function of the number of aggregated grid points shows that the ratio decreases with mean correlation between the aggregated points and approaches $\sqrt{R}$ as the number of aggregated points increases to ∞. A significant result of this analysis is that the benefit of aggregation saturates beyond 10 grid points. It is to be noted that this study looks at the nature of the geophysical resource irrespective of the technologies adopted for harvesting and integrating the generated power into the grid.

The variations in the electrical load are largely assumed to be statistically independent. Thus, it is argued that similar variations in wind generation are also statistically independent and hence these variations in wind generation are assumed to have no net impact on electrical generation [4]. But, although the small scale variations (second to minute scale) in the electrical load are random and hence statistically independent, the variations that occur at larger scale are not random but deterministic. For instance, the large increase in electric demand in the morning and evening and those occurring due to wide-spread low or high atmospheric temperatures are not statistically independent and are deterministic and load variations in a region are correlated. Similarly, the small scale variations in wind generation may be statistically independent, but the variations at the time scales of hour and greater are meteorologically forced.

This analysis has several significant implications for harvesting and aggregation of wind power in the United States. Reliability of wind power systems requires steady aggregated wind power. While planning interconnects of power like those in the Eastern Wind Integration and Transmission Study (EWITS) [5], it is important to exclude the grid points that have strongly falling generation duration curves. Back up power from gas power plants needs to be planned for the times when the ISO regions lose wind power. But, if several ISO regions lose wind power at the same time, as shown above, the amount of back up power required may be very high. Lastly, the magic number of 10 grid points as the limit of the number of grid points that can be optimally aggregated implies that the ten grid points with the least mean correlation among them in each ISO region need to be aggregated, since any further aggregation from other points does not improve the variability of the wind resource. For mitigation of the residual intermittency, other strategies, like high efficiency and high capacity storage, need to be devised. Since the correlation of collocated solar and wind power is also low, such hybrid harvesting may also be a viable strategy for reliable power [24].

Wind power harvested in large scale, usually, is not utilized in isolation but only forms a component in the energy mix of a region or country. Since the abundance of the newly discovered gas reserves in the US and the ability of gas powered plants to switch fast in response to demand are seen as one of the viable tools to mitigate wind power variability and intermittency. This study, in this context, attempts to understand the aggregated wind power so that the levelized costs of wind power can be further reduced and the contribution of the cycling of the gas power plants to greenhouse gas emissions can further be reduced.

Acknowledgments

Appendix A. Detailed description of the data and the methodology

A.1. Dataset

Wind power density as a variable that describes the wind resource has been constructed using the Modern Era Retrospective-analysis for Research and Applications dataset. The geographic region considered is bounded by 20–50° N and 130–60° W. The spatial resolution of the grid is 1/2° latitude × 2/3° longitude. Boundary layer flux data (friction velocity, roughness length and displacement height) have been used to derive the wind speed at 80 m by applying the similarity theory for the boundary layer. Thus, instead of assuming a scaling or adjustment procedure to estimate the wind speed at 80 m from the wind speed at a lower altitude, our procedure computes the wind speed at 80 m. One of the problems with the former procedure, which is widely used, is that it does not take the roughness length and displacement height of the boundary layer into account and leads to large errors in the estimate of wind speeds at a higher altitude [18]. Using the air density and the wind speed computed as above, the wind power density is computed. Since it takes into account the changes in air density, it is a more robust measure of wind resource. The constructed resource has been validated by comparing with the US wind atlas at 80 m developed by the National Renewable Energy Laboratory. Further, the method has been used to construct wind resource for Europe [25], Australia [26] and South Africa [27]. The constructed estimates have been compared with the wind atlases of the respective regions or the countries.

A.2. Turbine size

From the wind power density time series at each grid point, the hourly wind power generated at each grid point is computed. To estimate the power generated, a number of GE 1.5SLE wind turbines are assumed to be installed at each grid point. The power curve of this turbine (shown in Fig. A.6) has been converted from a function of wind speed into a function of wind power density. This transformed power curve has been used to compute the power produced by this turbine each hour.

A.3. Number of turbines

Wake effects reduce the wind speed for the subsequent rows of turbines. Thus, these wake effects have to be considered to compute the power generated by an array of wind turbines. Based on turbulence studies of the boundary layer and the wind turbines, it was found that placing wind turbines 15 rotor diameters is most cost-effective for power generation. Using this assumption, the density of wind turbines for optimum power generation is about 3 turbines per square kilometer. Considering the constraints on land uses, it is assumed that 1% of each grid cell area, on average, could be reasonably be used for power generation. We bring to the notice of the reader that we use non-dimensionalized quantities in our experiments and so, this proportion of land for deployment of wind turbines is extraneous for the present study.

Using these assumptions, the hourly wind power generated in each grid cell is computed. The power generated in each grid cell falling into each ISO is aggregated. The ratio of the aggregated power at each hour to the rated power gives the aggregated capacity factor (ACF) for each ISO.

Appendix B. Statistics of intermittency

In this section, we treat the dependence of the variability of wind generation on the correlation between the generating units analytically. This treatment follows approximately, the portfolio theory. Suppose there are n wind power generating units with mean output power $\overline{p_1}, \overline{p_2}, \overline{p_3}, \ldots, \overline{p_n}$ and mean fluctuations $p'_1, p'_2, p'_3, \ldots, p'_n$. The aggregated power from these n units is:

$$\overline{P} = (\overline{p_1} + \overline{p_2} + \overline{p_3} + \cdots + \overline{p_n}) + (p'_1 + p'_2 + p'_3 + \cdots + p'_n) \quad \text{(B.1)}$$

at each hour and the mean squared deviation is:

$$\overline{P'^2} = (p'^2_1 + p'^2_2 + p'^2_3 + \cdots + p'^2_4)$$
$$+ 2(\overline{p'_1 p'_2} + \overline{p'_2 p'_3} + \cdots + \overline{p'_{n-1} p'_n}) \quad \text{(B.2)}$$

Now, to simplify the treatment, let us assume that:

1. each unit has the same mean power p_m and
2. each unit has the same fluctuation p_f.

Therefore,

$$\overline{P'^2} = np_f^2 + 2(\overline{p'_1 p'_2} + \overline{p'_2 p'_3} + \cdots + \overline{p'_n p'_{n-1}})$$
$$= np_f^2 + n(n-1)Rp_f^2 \quad \text{(B.3)}$$

where R is the mean correlation coefficient between every pair of generating units.

Letting $p' = \sqrt{\overline{P'^2}}$, the coefficient of variation of the aggregate power is given by:

$$\text{CoV} = \frac{p'}{P} = \frac{\sqrt{np_f^2 + n(n-1)Rp_f^2}}{np_m} \quad \text{(B.4)}$$

B.1. Case 1: no correlation

Let us assume there is no correlation between the units. Then, the second term in the square root above is zero. Therefore,

$$\text{CoV}_1 = \frac{\sqrt{n}p_f}{np_m} = \frac{1}{\sqrt{n}} \frac{p_f}{p_m} \quad \text{(B.5)}$$

B.2. Case 2: positive correlation

Now let us assume a common correlation coefficient of R between every pair of units. Thus, the coefficient of variation becomes:

$$\text{CoV}_2 = \frac{p_f}{p_m} \frac{\sqrt{n + n(n-1)R}}{n} \quad \text{(B.6)}$$

where $\frac{p_f}{p_m}$ is the coefficient of variation of the individual units. Fig. 5 in the main paper shows the variation of the ratio of CoV_2 and CoV_1 with the number of wind generating units that are aggregated and the coefficient of correlation R is a parameter. This plot shows that for the initial 10 units, the reduction in CoV is drastic and for subsequent addition of each unit, the benefit of aggregation is marginal. More importantly, as the correlation between the units increases, the benefit of aggregation saturates faster, that is with fewer number of turbines. This plot also shows that with even a correlation of 0.3, the reduction in the coefficient of variation becomes almost half of that with no correlation. It can be shown that the limit of the ratio of CoV_2 and CoV_1 as the number of the generating units increases asymptotically approaches $\sqrt{R}$.

References

[1] NREL. 20% Wind Energy by 2030, Technical Report DOE/GO-102008-2567, National Renewable Energy Laboratory (NREL)., Golden, CO.; 2008. doi:http://dx.doi.org/10.2172/937007.

[2] George S, George H, Nguyen S. Risk quantification associated with wind energy intermittency in california. IEEE Trans Power Syst 2011;26(4):1937–44. http://dx.doi.org/10.1109/TPWRS.2011.2118239.

[3] MIT Energy Initiative. Managing large-scale penetration of intermittent renewables, Technical Report, Massachusetts Institute of Technology, Cambridge, Massachusetts, USA; 2011.

[4] Milligan M, Porter K, DeMeo E, Denholm P, Holttinen H, Kirby B, et al. Wind power myths debunked. IEEE Power Energy Mag 2009;7(6):89–99.

[5] Corbus D, King J, Mousseau T, Zavadil R, Heath B, Hecker L, Lawhorn J, Osborn D, Smith J, Hunt R, Moland G. Eastern Wind Integration and Transmission Study, Technical Report NREL/SR-550-47078, Prepared for NREL by EnerNex Corporation, Knoxville, Tennessee; 2011.

[6] MacKay DJ. Sustainable energy – without the hot air. 1st ed. UIT Cambridge Ltd.; 2009.

[7] Holttinen H, Meibom P, Orths A, Lange B, O'Malley M, Tande J, et al. Impacts of large amounts of wind power on design and operation of power systems, results of IEA collaboration. Wind Energy 2011;14(2):179–92.

[8] Kirby B, Milligan M. Facilitating wind development: the importance of electric industry structure. Electr. J. 2008;21(3):40–54. http://dx.doi.org/10.1016/j.tej.2008.03.001. <http://www.sciencedirect.com/science/article/pii/S1040619008000535>.

[9] ISO/RTO Council. Map – ISO/RTO council. <http://www.isorto.org/site/c.jhKQIZPBImE/b.2604471/k.B14E/Map.htm>; 2013 (accessed on 07.13.13).

[10] NREL. Wind powering America: 80-Meter wind maps and wind resource potential. <http://www.windpoweringamerica.gov/wind_maps.asp>; 2010 (accessed on 22.06.11).

[11] Monteiro C, Bessa R, Miranda V, Botterud A, Wang J, Conzelmann G, Porto I, et al., Wind power forecasting: state-of-the-art 2009. Tech. rep., Argonne National Laboratory (ANL); 2009.

[12] Farkas Z. Considering air density in wind power production. Arxiv preprint arXiv:1103.2198.

[13] Elliott DL, Holladay CG, Barchet WR, Foote HP, Sandusky WF. Wind energy resource atlas of the united states, NASA STI/Recon Technical Report N 1987; 87: p. 24819.

[14] Archer CL, Jacobson MZ. Supplying baseload power and reducing transmission requirements by interconnecting wind farms. J Appl Meteorol Climatol 2007;46(11):1701–17.

[15] Katzenstein W, Fertig E, Apt J. The variability of interconnected wind plants. Energy Policy 2010;38(8):4400–10.

[16] Lu X, McElroy MB, Kiviluoma J. Global potential for wind-generated electricity. Proc Nat Acad Sci 2009;106(27):10933–8.

[17] Archer CL, Jacobson MZ. Spatial and temporal distributions of US winds and wind power at 80 m derived from measurements. J Geophys Res 2003;108(D9):42–89.

[18] Pryor S, Barthelmie R. Assessing climate change impacts on the near-term stability of the wind energy resource over the united states. Proc Nat Acad Sci 2011;108(20):8167.

[19] Gunturu UB, Schlosser CA. Characterization of wind power resource in the United States. Atmos Chem Phys 2012;12(20):9687–702. http://dx.doi.org/10.5194/acp-12-9687-2012. <http://www.atmos-chem-phys.net/12/9687/2012/>.

[20] Rienecker MM, Suarez MJ, Gelaro R, Todling R, Bacmeister J, Liu E, et al. MERRA: NASA's Modern-Era retrospective analysis for research and applications. J Climate 2011;24:3624–48. http://dx.doi.org/10.1175/JCLI-D-11-00015.1.

[21] Meyers J, Meneveau C. Optimal turbine spacing in fully developed wind farm boundary layers. Wind Energy 2012;15(2):305–17. http://dx.doi.org/10.1002/we.469.

[22] Barriopedro D, García-Herrera R, Lupo AR, Hernández E. A climatology of northern hemisphere blocking. J. Clim. 2006;19(6):1042–63.

[23] Stocker TF, Qin D, Plattner GK, Tignor M, Allen SK, Boschung J, Nauels A, Xia Y, Bex B, Midgley BM. IPCC, 2013: climate change 2013: the physical science basis. Contribution of working group I to the fifth assessment report of the intergovernmental panel on climate change. Cambridge University Press; 2013.

[24] Widen J. Correlations between large-scale solar and wind power in a future scenario for Sweden. IEEE Trans Sustain Energy 2011;2(2):177–84. http://dx.doi.org/10.1109/TSTE.2010.2101620.

[25] Cosseron A, Gunturu UB, Schlosser CA. Characterization of the wind power resource in Europe and its intermittency. Energy Procedia 2013;40:58–66.

[26] Hallgren W, Gunturu UB, Schlosser A. The potential wind power resource in australia: a new perspective. PLoS One 2014;9(7):e99608. http://dx.doi.org/10.1371/journal.pone.0099608.

[27] Fant C, Gunturu UB. Characterizing wind power resource reliability in southern africa, WIDER Working Paper 2013/067, Helsinki. <http://hdl.handle.net/10419/80951>; 2013.

[28] GE-Energy, GE Energy: 1.5 - 77 Wind Turbine, <http://www.ge-energy.com/products_and_services/products/wind_turbines/ge_1.5_77_wind_turbine.jsp>; 2013 (accessed on 07.13.13).

MIT Joint Program on the Science and Policy of Global Change - REPRINT SERIES

2014-7   Potential Influence of Climate-Induced Vegetation Shifts on Future Land Use and Associated Land Carbon Fluxes in Northern Eurasia, Kicklighter, D.W., Y. Cai, Q. Zhuang, E.I. Parfenova, S. Paltsev, A.P. Sokolov, J.M. Melillo, J.M. Reilly, N.M. Tchebakova and X. Lu, *Environmental Research Letters,* 9(3): 035004 (2014)

2014-8   Implications of high renewable electricity penetration in the U.S. for water use, greenhouse gas emissions, land-use, and materials supply, Arent, D., J. Pless, T. Mai, R. Wiser, M. Hand, S. Baldwin, G. Heath, J. Macknick, M. Bazilian, A. Schlosser and P. Denholm, *Applied Energy,* 123(June): 368–377 (2014)

2014-9   The energy and CO$_2$ emissions impact of renewable energy development in China, Qi, T., X. Zhang and V.J. Karplus, *Energy Policy*, 68(May): 60–69 (2014)

2014-10   A framework for modeling uncertainty in regional climate change, Monier, E., X. Gao, J.R. Scott, A.P. Sokolov and C.A. Schlosser, *Climatic Change,* online first (2014)

2014-11   Markets versus Regulation: The Efficiency and Distributional Impacts of U.S. Climate Policy Proposals, Rausch, S. and V.J. Karplus, *Energy Journal*, 35(SI1): 199–227 (2014)

2014-12   How important is diversity for capturing environmental-change responses in ecosystem models? Prowe, A. E. F., M. Pahlow, S. Dutkiewicz and A. Oschlies, *Biogeosciences*, 11: 3397–3407 (2014)

2014-13   Water Consumption Footprint and Land Requirements of Large-Scale Alternative Diesel and Jet Fuel Production, Staples, M.D., H. Olcay, R. Malina, P. Trivedi, M.N. Pearlson, K. Strzepek, S.V. Paltsev, C. Wollersheim and S.R.H. Barrett, *Environmental Science & Technology*, 47: 12557–12565 (2013)

2014-14   The Potential Wind Power Resource in Australia: A New Perspective, Hallgren, W., U.B. Gunturu and A. Schlosser, *PLoS ONE,* 9(7): e99608, doi: 10.1371/journal.pone.0099608 (2014)

2014-15   Trend analysis from 1970 to 2008 and model evaluation of EDGARv4 global gridded anthropogenic mercury emissions, Muntean, M., G. Janssens-Maenhout, S. Song, N.E. Selin, J.G.J. Olivier, D. Guizzardi, R. Maas and F. Dentener, *Science of the Total Environment,* 494-495(2014): 337-350 (2014)

2014-16   The future of global water stress: An integrated assessment, Schlosser, C.A., K. Strzepek, X. Gao, C. Fant, É. Blanc, S. Paltsev, H. Jacoby, J. Reilly and A. Gueneau, *Earth's Future,* 2, online first (doi: 10.1002/2014EF000238) (2014)

2014-17   Modeling U.S. water resources under climate change, Blanc, É., K. Strzepek, A. Schlosser, H. Jacoby, A. Gueneau, C. Fant, S. Rausch and J. Reilly, *Earth's Future,* 2(4): 197–244 (doi: 10.1002/2013EF000214) (2014)

2014-18   Compact organizational space and technological catch-up: Comparison of China's three leading automotive groups, Nam, K.-M., *Research Policy*, online first (doi: 10.1002/2013EF000214) (2014)

2014-19   Synergy between pollution and carbon emissions control: Comparing China and the United States, Nam, K.-M., C.J. Waugh, S. Paltsev, J.M. Reilly and V.J. Karplus, *Energy Economics*, 46(November): 186–201 (2014)

2014-20   The ocean's role in the transient response of climate to abrupt greenhouse gas forcing, Marshall, J., J.R. Scott, K.C. Armour, J.-M. Campin, M. Kelley and A. Romanou, *Climate Dynamics*, online first (doi: 10.1007/s00382-014-2308-0) (2014)

2014-21   The ocean's role in polar climate change: asymmetric Arctic and Antarctic responses to greenhouse gas and ozone forcing, Marshall, J., K.C. Armour, J.R. Scott, Y. Kostov, U. Hausmann, D. Ferreira, T.G. Shepherd and C.M. Bitz, *Philosophical Transactions of the Royal Society A*, 372: 20130040 (2014).

2014-22   Emissions trading in China: Progress and prospects, Zhang, D., V.J. Karplus, C. Cassisa and X. Zhang, *Energy Policy,* 75(December): 9–16 (2014)

2014-23   The mercury game: evaluating a negotiation simulation that teaches students about science-policy interactions, Stokes, L.C. and N.E. Selin, *Journal of Environmental Studies & Sciences*, online first (doi:10.1007/s13412-014-0183-y) (2014)

2014-24   Climate Change and Economic Growth Prospects for Malawi: An Uncertainty Approach, Arndt, C., C.A. Schlosser, K.Strzepek and J. Thurlow, J*ournal of African Economies,* 23(Suppl 2): ii83–ii107 (2014)

2014-25   Antarctic ice sheet fertilises the Southern Ocean, Death, R., J.L.Wadham, F. Monteiro, A.M. Le Brocq, M. Tranter, A. Ridgwell, S. Dutkiewicz and R. Raiswell, *Biogeosciences*, 11, 2635–2644 (2014)

2014-26   Understanding predicted shifts in diazotroph biogeography using resource competition theory, Dutkiewicz, S., B.A. Ward, J.R. Scott and M.J. Follows, *Biogeosciences,* 11, 5445–5461 (2014)

2**014-27   Coupling the high-complexity land surface model ACASA to the mesoscale model WRF,** L. Xu, R.D. Pyles, K.T. Paw U, S.H. Chen and E. Monier, *Geoscientific Model Development*, 7, 2917–2932 (2014)

2015-1   Double Impact: Why China Needs Separate But Coordinated Air Pollution and CO$_2$ Reduction Strategies, Karplus, V.J., *Paulson Papers on Energy and Environment* (2015)

2015-2   Behavior of the aggregate wind resource in the ISO regions in the United States, Gunturu, U.B. and C.A. Schlosser, *Applied Energy*, 144(April): 175–181 (2015)